Microchemical Journal 200 (2024) 110281

Contents lists available at ScienceDirect

Microchemical Journal

journal homepage: www.elsevier.com/locate/microc

The impact of formalin fixation in the elemental content of tissues: Parametrization up to 48 h

João Silva [a,b], Ricardo Castelhano [a], Fernanda Silva [c], José Paulo Santos [a,b], Ana Félix [c,d], João Cruz [a,b], Jorge Machado [a,b], Sofia Pessanha [a,b,*]

[a] NOVA School of Science and Technology, Campus Caparica, 2829-516, Caparica, Portugal
[b] LIBPhys, Laboratory of Instrumentation, Biomedical Engineering and Radiation Physics, LA-REAL
[c] NOVA Medical School, Campo dos Mártires da Pátria 130, 1169-056 Lisboa
[d] Instituto Português de Oncologia de Lisboa Francisco Gentil (IPOLFG)

A B S T R A C T

Formalin fixation is a crucial step in the preparation of tissue samples for anatomic pathology studies, however, research showed that prolonged formalin fixation, can alter the elemental composition of tissues with implications for pathology and biomedical research. In this study we aim to assess and parametrize the influence of short-term formalin fixation in tissues.

Six sets of human colon tissue samples were exposed to different formalin fixation times, up until 48 h. The elemental content throughout time was compared to the elemental content of the snap-frozen sample of the same tissue that was not exposed to formalin using Energy Dispersive X-ray Fluorescence.

Results showed a clear decrease of Cl and K concentration in the tissues solution reaching a plateau between 1 h and 3 h of fixation. Also, there is an uptake of P in the tissue, likely due to the buffered formalin solution, within the first 15 min of fixation. This behaviour was concomitant with an increase of Na determined using Particle Induced gamma-ray emission analysis (PIGE) and Elastic Backscattering Spectroscopy (EBS). The dynamic changes determined in the studied elements demonstrate that a better understanding of the fixation-related mechanisms is in demand as well as optimization of the fixation protocols implemented in anatomic pathology laboratories.

1. Introduction

In oncology every time a biological sample is removed, the total (surgical specimen) or a portion (biopsy) of normal and tumour tissue is retrieved and processed as formalin fixed paraffin embedded (FFPE) blocks for diagnosis and afterwards they are stored for safekeeping. Formalin fixation is a critical step in the preparation of tissue samples for anatomic pathology studies, it helps to preserve tissue architecture and cell composition in tissues, and additionally to allow them to withstand subsequent processing. Fixation also preserves all cell components such as the proteins and carbohydrates in their spatial relationship to the cell, so that they can be studied [1].

Considering the indubitable contribution of trace elements to the understanding of carcinogenesis [2–10], there is a need to harvest elemental information on FFPE tissue blocks, for a comprehensive and statistically meaningful investigation. These studies will allow establishing possible correlations between the various elements and factors like age, sex, diagnosis and stage of disease. Atomic spectrometry techniques have been attempted previously in the analysis of such samples, namely, for the analysis of elemental content in cancer tissue by synchrotron micro X-ray Fluorescence [11] as well as correlating with other prognostic factors [12], or by using inductively coupled plasma mass-spectrometry for the analysis of iron, zinc, selenium and cadmium in prostate tissue specimens [13]. The analysis of these *FFPE* samples has also been performed on the comparison of paired normal-tumour samples of breast and colon biopsied tissues using 2D-EDXRF. Moreover, potential of de-paraffinization and re- paraffinization was evaluated using Total-reflection X-ray Fluorescence [14] and synchrotron radiation [15].

However, a recent study by Pessanha et al. [16] demonstrated that formalin fixation, in periods longer than 48 h, alters permanently the elemental composition of Cl and K in tissues. This eradication of K and Cl from tissues due to formalin, constraints the analysis of Formalin Fixed Paraffin Embedded tissue blocks or other samples preserved with this solution, as these elements are potential biomarkers for pathologies, namely, cancer: Chloride intracellular channel 1 (CLIC1), member of the chloride intracellular channel family, has been proposed as a potential biomarker for various types of cancer due to its involvement in various

* Corresponding author.
E-mail address: sofia.pessanha@fct.unl.pt (S. Pessanha).

https://doi.org/10.1016/j.microc.2024.110281
Received 24 November 2023; Received in revised form 9 February 2024; Accepted 1 March 2024
Available online 5 March 2024

physiological functions, including regulation of cell volume, organelle acidification and modulation of ion homeostasis [17] CLIC1 expression appears ubiquitous in many human cancer tissues where it has been reported to act as an oncogene [18].

Potassium, on the other hand, is the most abundant cation in the intracellular fluid and it plays a vital role in the maintenance of normal cell functions as both oxidative stress (OS) and potassium imbalance can cause serious health conditions [19]. In carcinogenesis, alterations in K^+ channel function can promote the acquisition of the so-called hallmarks of cancer – cell proliferation, resistance to apoptosis, metabolic changes, angiogenesis, and migratory capabilities [20].

Considering the relevance of these elements as well as the importance of gauging information on FFPE tissue samples stored in the pathology departments in Hospitals throughout the world, we aim at parametrizing the elemental alterations in formalin fixed tissues, up until 48 h of fixation, using Energy Dispersive X-ray Fluorescence.

2. Materials and methods

2.1. Human tissues

Samples were obtained from Instituto Português de Oncologia de Lisboa, Francisco Gentil (IPOLFG). Colon samples were collected from 6 different patients, that have signed an informed consent to authorize their collection for research. This specific study was authorized and approved by the Ethics Committee of IPOLFG (UIC/1417), and all experiments were performed under the guidelines and regulations for handling human tissues. Samples (cold ischemia < 10 min) were collected from 6 surgical specimens and divided into 9 cubes with approximately 1 cm^3: one portion of each set was snap-frozen, and the remaining portions were preserved in a 10 % v/v formalin buffered solution (4 % formaldehyde stabilized with methanol 0.5–1.5 %, VMR Chemicals, USA) until removal from the vials, according to different time-frames, up until 48 h. Only adjacent normal healthy tissue was selected for this research.

Samples were removed from the vials, washed with distilled water to remove excess formalin, and freeze-dried using a Modulyo Freeze Dryer system (Edwards, UK), operated at −60 °C and 20 Pa during 48 h.

The lyophilized samples were powdered using a pestle and mortar, and a mechanical mill. The obtained powder was pressed into pellets, 1.5–1.7 mm thick, that were glued onto a Mylar film and placed on a slide frame. Each tissue cube rendered only one pellet.

2.2. Experimental setup – micro-Energy Dispersive X-ray Fluorescence system

EDXRF analysis of the samples was performed with a benchtop micro energy dispersive X- ray fluorescence (μ-EDXRF) system, the M4 TORNADO (Bruker, Germany). This spectrometer system uses poly-capillary X-ray optics with spot size of 25 μm for Mo − Kα radiation. The excitation of samples is achieved with a Peltier-cooled X-ray tube with a Rh target, and the detection is achieved with a silicon drift detector (SDD) that has a sensitive area of 30 mm^2 and 13 μm thick Be window and energy resolution 145 eV for the Kα line of Mn. The X- ray tube was operated at 50 kV, 300 μA, 12.5 μm Al filter, and 20 mBar vacuum inside the system's chamber.

2D scans of 1x1 mm^2 of the samples were performed with a 35 μm step and a time per step of 10 ms/pixel. Each 2D frame was repeated 5 times yielding an acquisition time of, approximately, 1 min. Three scans were performed for each pellet.

2.2.1. Quantification method and validation

Elemental quantification was performed using MQuant, the in-built software of the M4 TORNADO system. It allows spectra deconvolution, peak fitting, and quantification using the Fundamental Parameters (FP) method based on Sherman's equation and the following matrix composition, was provided ad-hoc to the software (10 % - H, 22 % - C, 3 % - N, and 60 % - O [21]). Limits of Detection (LoD), Limits of Quantification (LoQ) and validation results for the reference material Oyster Tissue SRM 1566 are presented in Pessanha et al. [16]. For the elements evaluated using this experimental technique (P, S, Cl, K, Ca, Fe, Cu and Zn).

Table 1
Mean, standard deviation, minimum and maximum obtained values (μg/g) for P, S, Cl, Ca, Fe and Zn in the analyzed snap-frozen samples.

	Mean	Standard Deviation	Minimum	Maximum	Coefficient of variance (%)
P	4000	1200	2161	5898	31
S	5100	550	3704	6131	11
Cl	10,000	2000	7010	13,750	20
K	6400	1200	4144	8409	19
Ca	400	200	168	914	54
Fe	24	10	10	45	45
Zn	11	4	4	18	38

2.3. Particle Induced Gama-Ray emission (PIGE) setup

The experimental work for PIGE was carried out at the IST/CTN 3 MV Tandem accelerator, using 2.8 MeV proton beam. Before entering the reaction chamber, the beam passes through a collimator which defines a beam spot of around 2 mm on the sample, allowing, in this case, two or three different spots per sample to be analysed. The 440 keV gamma-rays from the $^{23}Na(p, p'\gamma)^{23}Na$ nuclear reactions, were detected by a 45 % Ge(HP) detector located at 130° in relation to the incident beam direction. The net areas of the gamma-ray peaks were obtained by an automatic peak analyzer script in the OriginPro software (v.9.9.0.225 OriginLab Corporation, USA) which was able to fit the peaks to a Gauss curve.

2.3.1. Quantification method and validation

The result validation for the PIGE analysis of Na was achieved by the means of Elastic Backscattering spectra analysis of the studied samples. The backscattered protons were detected by a PIPS® (Passivated Implanted Planar Silicon, Camberra), present in the nuclear reaction chamber. The IBA DataFurnace (NDF) [22], was used to simulate the atomic mass fractions of each element in the sample in order to best fit each spectrum. The atomic mass fraction of hydrogen was set to 63 %, and since the RBS technique is not sensitive to this element, the collected charge for each simulation was tweaked to offset any deviations from the hydrogen matrix composition values of the tissue samples. After a satisfactory fitting for each EBS spectrum, the atomic mass fractions of each element in the sample and the simulated collected charge were used as parameters in a standard free method for PIGE in thick samples, based on the ERYA (Emitted Radiation Yield Analysis) code [23], in order to quantify sodium.

2.4. Statistical analysis

Statistical analysis was performed using OriginPro software (v.9.9.0.225 OriginLab Corporation, USA). The normality of the distributions of each of the studied elements was tested with the Shapiro-Wilk Test. Since not all elements in all samples were normally distributed, non-parametric Kruskal-Wallis Test was used to test for differences between fixation times. Furthermore, k-means cluster analysis was performed to understand the behaviour of elements such as Ca, S, Fe and Zn.

3. Results

Table 1 presents the descriptive statistics obtained for snap-frozen tissue samples. As can be seen, the coefficient of variance, indicative of the variation of values within populations ranges between 11 % for S

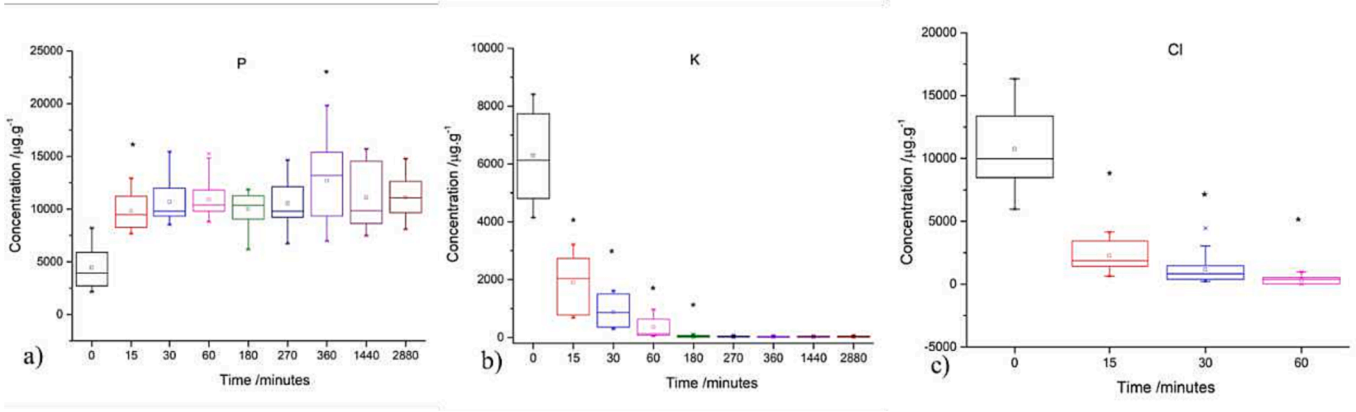

Fig. 1. Box-plot charts for the elemental composition of a) P, b) K and c) Cl in the different tissues sets. * marks significant differences from the previous timeframe.

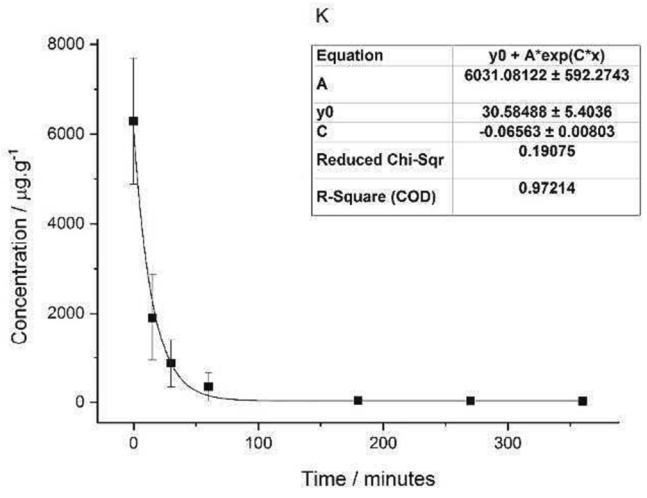

Fig. 2. Variation of the mean elemental content of K with fixation time.

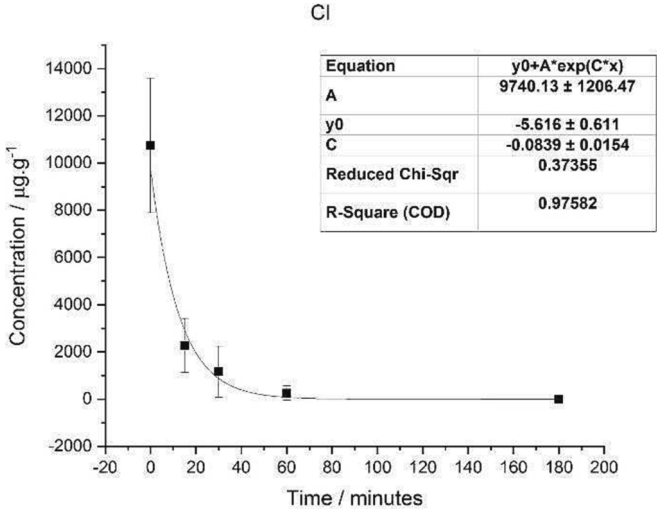

Fig. 3. Variation of the mean elemental content of Cl with fixation time.

to 54 % for Ca. This is indicative of the intrinsic biological variability of the elemental concentrations of minor and trace elements in biological tissues [24,25].

In Fig. 1 are presented the box-plot charts with the variations of concentration of P, K and with time of fixation in formalin. As can be

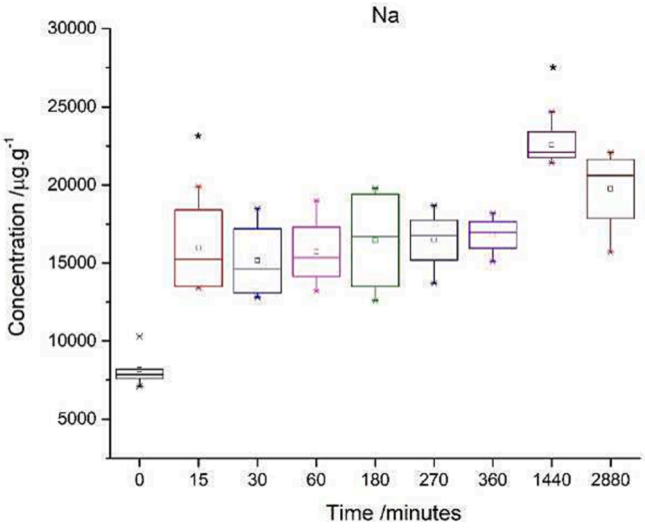

Fig. 4. Box-plot charts for the elemental composition of Na in the different tissues sets. * marks significant differences from the previous timeframe.

seen, there is a significantly different increase ($p < 0.001$) in P concentration over the 15 min exposure to formalin (over 120 % increase), but the concentration remained not significantly different until 48 h (2440 min). Regarding K and Cl, as expected, the concentration decreased drastically upon 48 h fixation in formalin. Statistical analysis revealed significant differences until 180 min exposure, but after this fixation time in formalin the concentration of Cl was below detection limit (BDL), while K was reduced to less than 50 µg/g. Fig. 2

In order to evaluate the rate of decrease of K and Cl with time in formalin, exponential functions were fitted to the curves obtained from plotting the mean elemental concentration (for the 6 sets of tissues) as a function of time. As can be seen the rate of decay is slightly different for both elements and higher for Cl (Fig. 3).

Conversely to the K and Cl profiles and concomitant with P, Na presented an increasing behaviour, with significant increase after 15 min of fixation (95 % increase) and again after 24 h of fixation (34 % increase) (Fig. 4).

Regarding the other elements present in the tissues, Fig. 5 presents the boxplot charts obtained for the different fixation times. As can be seen from the charts there is no overall significant decrease due to the exposure to formalin, however, significant differences were found between some fixation times, marked in the box-plot chart with an asterisk.

To further understand if the differences are due to formalin fixation or sample biological variability, k-means cluster analysis was performed

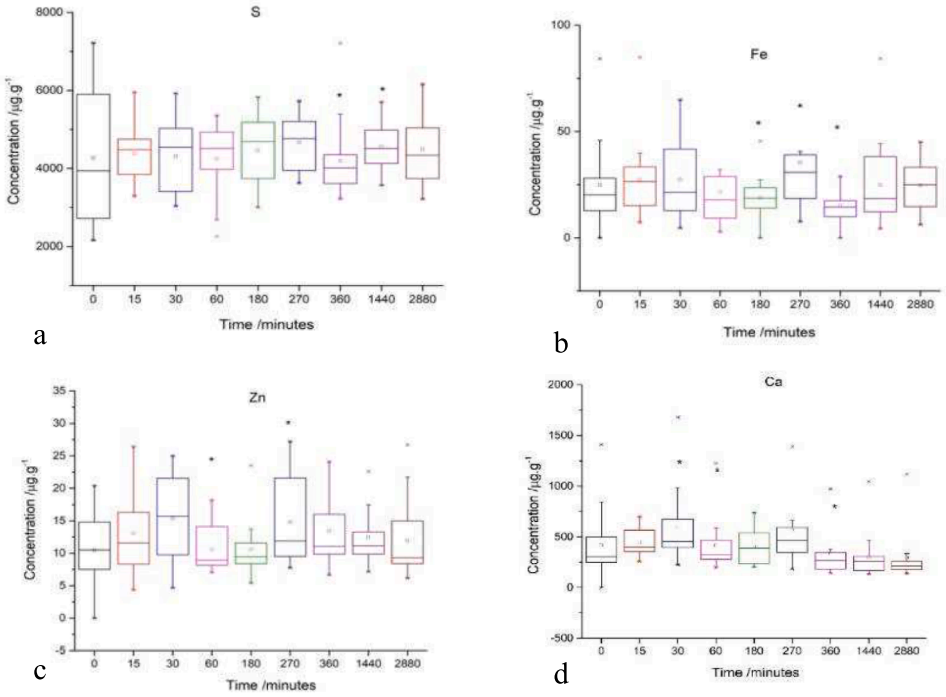

Fig. 5. Box-plot charts for the elemental composition of S, Fe, Zn and Ca in the different tissues sets. * marks the timeframes where significant differences were found.

Table 2
Distribution of points per cluster (%) considering the concentration of S, Ca, Fe and Zn.

Time in formalin (minutes)	Cluster 1	Cluster 2	Cluster 3	Cluster 4
0	9	32	45	14
15	47	0	24	29
30	45	5	35	15
60	45	0	18	36
180	61	0	17	22
270	39	17	0	44
360	18	5	23	55
1440	44	6	0	50
2880	22	17	17	44

on the quantitative determinations for these 4 elements. Table 2 shows the distribution of measured spectra in each cluster, and Fig. 6 presents the cluster plot considering Ca, S, Fe and Zn. Results showed the formation of 4 different clusters regarding the plotted elements, however, the clustering was independent of the time in formalin, and much more dependent of the S content as can be seen from the distribution of events in the 4 clusters. The S concentration in these tissues presented a large intrinsic variability, consistent with literature found for colon samples [4,24].

4. Discussion

The main role of formalin fixation is to preserve the morphology (structure) of the tissue sample. Without fixation, tissue samples can quickly degrade (autolysis) and become distorted, making it difficult or impossible to accurately interpret the morphology and perform a diagnosis.

Formalin fixation also helps to prevent heterolysis, the process by which cells in the tissue begin to break down after death, making the tissue safer to handle and reduces the risk of contamination.

The results of this study demonstrate the impact of formalin fixation time on the elemental composition of tissue samples, specifically regarding Na, P, K and Cl concentrations. Rapid uptake in P and Na, from the buffered formalin solution was observed within the first 15 min

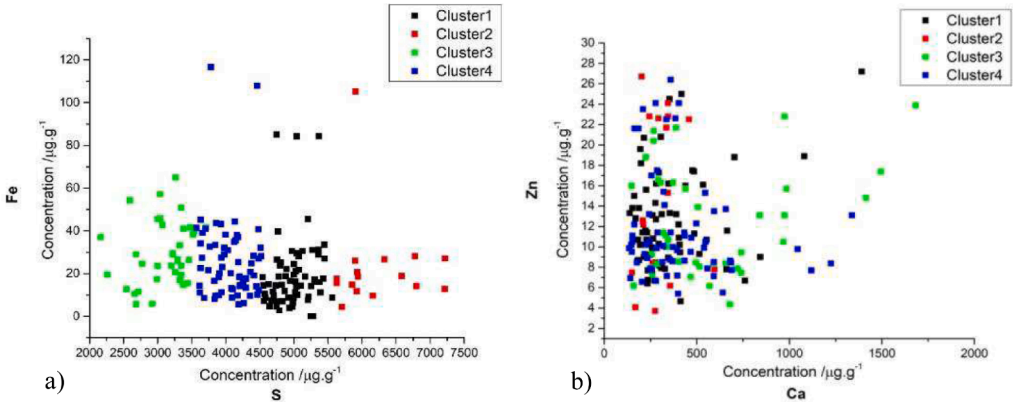

Fig. 6. K-means cluster plots for S, Fe, Ca and Zn.

of fixation. Evidence of the presence of P in the solution was presented by Pessanha et al. [16] when comparing the composition of a micro-carry® paper filter (Rigaku, Japan) before and after spiking with clear formalin solution. Additional PIGE analysis of the same paper filters showed a 3.18-fold increase of Na signal after spiking with formalin. Conversely, prolonged fixation can lead to leaching or loss of K and Cl from tissues with concentrations decreasing significantly to levels within the Limit of Detection of the technique after 48 h. The alterations in elemental composition can impact downstream analyses and interpretations, highlighting the need for optimized fixation protocols to ensure valid research findings and clinical diagnoses. The observed changes in elemental composition are linked to the activity of the Na + -K + -ATPase pump, which plays a vital role in maintaining cellular homeostasis. It actively transports sodium and potassium ions across the cell membrane against their concentration gradients. The pump utilizes ATP hydrolysis to move three sodium ions (Na +) out of the cell while transporting two potassium ions (K +) into the cell. This active transport mechanism helps maintain a higher concentration of sodium extracellularly and a higher level of potassium intracellularly, which is essential for cellular functioning [19]. These findings have implications for anatomy pathological procedures and cancer research, creating a need for comprehensive research on the impact of ischemia times in cell death [26,27] and establishment of improved standardized fixation protocols to preserve the integrity of Na, P, K and Cl as potential biomarkers.

5. Conclusion

This study demonstrated that K and Cl content in tissues decreases after short-time formalin fixation with concomitant increase of Na. These results show the direct impact of formalin fixation in tissues not avoiding the electrolytic changes due to cell death. It also highlights the important implications for the excellent fixation time protocols used in anatomic pathology procedures as well as other quantitative essays that rely on accurate measurement of elemental content. Protocols should be further standardized and fixation times optimized, taking into account these specific elemental changes and the understanding of these elemental changes may influence the design of experiments and the choice of fixation times. Researchers can make more informed decisions about the duration of fixation to minimize unwanted alterations in elemental composition.

CRediT authorship contribution statement

João Silva: Formal analysis, Data curation. **Ricardo Castelhano:** Formal analysis, Data curation. **Fernanda Silva:** Methodology. **José Paulo Santos:** Writing – original draft, Funding acquisition. **Ana Félix:** Writing – original draft, Methodology, Conceptualization. **João Cruz:** Formal analysis, Data curation. **Jorge Machado:** Conceptualization. **Sofia Pessanha:** Writing – original draft, Methodology, Conceptualization.

Declaration of competing interest

The authors declare that they have no known competing financial interests or personal relationships that could have appeared to influence the work reported in this paper.

Data availability

Data will be made available on request.

Acknowledgments

This work has been financially supported by Fundação para a Ciência e a Tecnologia through the LIBPhys funding UID/FIS/ 04559/2020, S. Pessanha contract CEECIND/00278/2018 and João Silva PhD grant BDANA/01513/2023.

References

[1] R. Thavarajah, V.K. Mudimbaimannar, J. Elizabeth, U.K. Rao, K. Ranganathan, Chemical and physical basics of routine formaldehyde fixation, journal of Oral and maxillofacial, Pathology 16 (2012) 400–405, https://doi.org/10.4103/0973-029X.102496.
[2] M.K. Schwartz, Role of trace elements in cancer | cancer research | American Association for Cancer Research, Cancer Res. 35 (1975) 3481–3487.
[3] M. Yaman, Comprehensive comparison of trace metal concentrations in cancerous and non-cancerous human tissues, Curr. Med. Chem. 13 (2006) 2513–2525, https://doi.org/10.2174/092986706778201620.
[4] S. Pessanha, D. Braga, A. Ensina, J. Silva, J. Vilchez, C. Montenegro, S. Barbosa, M. L. Carvalho, A. Dias, A non-destructive X-ray fluorescence method of analysis of formalin fixed-paraffin embedded biopsied samples for biomarkers for breast and colon cancer, Talanta 260 (2023) 124605, https://doi.org/10.1016/J.TALANTA.2023.124605.
[5] G.R. Monteith, D. McAndrew, H.M. Faddy, S.J. Roberts-Thomson, Calcium and cancer: targeting Ca2+ transport, Nature Reviews Cancer 2007 7:7. 7 (2007) 519–530. https://doi.org/10.1038/nrc2171.
[6] B.J. Grattan, H.C. Freake, Zinc and Cancer: Implications for LIV-1 in Breast Cancer, Nutrients 2012, Vol. 4, Pages 648-675. 4 (2012) 648–675. https://doi.org/10.3390/NU4070648.
[7] L. Jouybari, M.S.G. Naz, A. Sanagoo, F. Kiani, F. Sayehmiri, K. Sayehmiri, A. H. Dehkordi, Toxic elements as biomarkers for breast cancer: a meta-analysis study, Cancer Manag. Res. 10 (2018) 69–79, https://doi.org/10.2147/CMAR.S151324.
[8] D.O. Olaiya, O.I. Alatise, O.O. Oketayo, O.E. Abiye, E.I. Obianjunwa, F.A. Balogun, Trace element analysis of cancerous and non-cancerous breast tissues of african women in Southwest Nigeria using particle-induced X-ray emission technique, Breast Cancer (auckl.) 13 (2019), https://doi.org/10.1177/1178223419840694/ASSET/IMAGES/LARGE/10.1177_1178223419840694-FIG3.JPEG.
[9] S.J. Mulware, Comparative trace elemental analysis in cancerous and noncancerous human tissues using PIXE, Journal of Biophysics. 2013 (2013), https://doi.org/10.1155/2013/192026.
[10] O. Marques, B.M. da Silva, G. Porto, C. Lopes, Iron homeostasis in breast cancer, Cancer Lett. 347 (2014) 1–14, https://doi.org/10.1016/J.CANLET.2014.01.029.
[11] G.E. Falchini, A. Malezan, M.E. Poletti, E. Soria, M. Pasqualini, R.D. Perez, Analysis of phosphorous content in cancer tissue by synchrotron micro-XRF, Radiat. Phys. Chem. 179 (2021) 109157, https://doi.org/10.1016/J.RADPHYSCHEM.2020.109157.
[12] A. Al-Ebraheem, K. Geraki, R. Leek, A.L. Harris, M.J. Farquharson, The use of biometal concentrations correlated with clinical prognostic factors to assess human breast tissues, X-Ray Spectrom. 42 (2013) 330–336, https://doi.org/10.1002/XRS.2463.
[13] A.G. Sarafanov, T.I. Todorov, A. Kajdacsy-Balla, M.A. Gray, V. Macias, J. A. Centeno, Analysis of iron, zinc, selenium and cadmium in paraffin-embedded prostate tissue specimens using inductively coupled plasma mass-spectrometry, J. Trace Elem. Med Biol. 22 (2008) 305–314, https://doi.org/10.1016/J.JTEMB.2008.03.010.
[14] P.M. Wróbel, Ł. Chmura, P. Kasprzyk, K. Kozlowski, K. Wątor, M. Szczerbowska-Boruchowska, Feasibility study of elemental analysis of large population of formalin fixed paraffin embedded tissue samples – preliminary results, Spectrochim Acta Part B at Spectrosc. 173 (2020) 105971, https://doi.org/10.1016/J.SAB.2020.105971.
[15] A. Gianoncelli, K. Vogel- Mikuš, M. Salomé, E. Pascotto, G. Ricci, L. Pascolo, Difficulties and artefacts in cryo-fixation of ovarian tissues for X-ray fluorescence analyses, J. Anal. at. Spectrom 38 (2023) 1744–1750, https://doi.org/10.1039/D3JA00164D.
[16] S. Pessanha, A. Veiga, D. Doutel, F. Silva, J. Silva, P.M. Carvalho, S. Barbosa, J. P. Santos, A. Félix, J. Machado, Evaluation of the influence of the formalin fixation time on the elemental content of tissues measured with X-ray fluorescence, Spectrochim Acta Part B at Spectrosc. 205 (2023) 106704, https://doi.org/10.1016/J.SAB.2023.106704.
[17] H. Geng, C. Feng, Z. Sun, X. Fan, Y. Xie, J. Gu, L. Fan, G. Liu, C. Li, R.F. Thorne, X. D. Zhang, X. Li, X. Liu, Chloride intracellular channel 1 promotes esophageal squamous cell carcinoma proliferation via mTOR signalling, Transl. Oncol. 27 (2023) 101560, https://doi.org/10.1016/J.TRANON.2022.101560.
[18] Q. Ding, M. Li, X. Wu, L. Zhang, W. Wu, Q. Ding, H. Weng, X. Wang, Y. Liu, CLIC1 overexpression is associated with poor prognosis in gallbladder cancer, Tumor Biol. 36 (2015) 193–198, https://doi.org/10.1007/S13277-014-2606-5/METRICS.
[19] U.K. Udensi, P.B. Tchounwou, Potassium homeostasis, oxidative stress, and human disease, int J clin, Exp. Physiol. 4 (2017) 111, https://doi.org/10.4103/IJCEP.IJCEP_43_17.
[20] L. Zúñiga, A. Cayo, W. González, C. Vilos, R. Zúñiga, Potassium channels as a target for cancer therapy: current perspectives, Onco Targets Ther. 15 (2022) 783–797, https://doi.org/10.2147/OTT.S326614.
[21] A. Ensina, P.M. Carvalho, J. Machado, M.L. Carvalho, D. Casal, D. Pais, J.P. Santos, A.A. Dias, S. Pessanha, Analysis of human tissues using energy dispersive X ray fluorescence – dark matrix determination for the application to cancer research, J. Trace Elem. Med Biol. 68 (2021) 126837, https://doi.org/10.1016/J.JTEMB.2021.126837.

[22] N.P. Barradas, C. Jeynes, Advanced physics and algorithms in the IBA DataFurnace, Nucl Instrum Methods Phys Res b. 266 (2008) 1875–1879, https://doi.org/10.1016/J.NIMB.2007.10.044.
[23] V. Manteigas, M. Fonseca, A. Jesus, ERYA-Bulk | nuclear, (n.d.). https://sites.fct.unl.pt/nuclear/software/erya-bulk (accessed November 2, 2023).
[24] P.M. Carvalho, E. Marguí, A. Kubala-Kukuś, D. Banaś, J. Machado, D. Casal, D. Pais, J.P. Santos, S. Pessanha, Evaluation of different analytical approaches using total reflection X-ray fluorescence systems for multielemental analysis of human tissues with different adipose content, Spectrochim Acta Part B at Spectrosc. 198 (2022) 106548, https://doi.org/10.1016/J.SAB.2022.106548.
[25] U. Majewska, J. Braziewicz, D. Banaś, A. Kubala-Kukuś, S. Góźdź, M. Pajek, M. Zadrozna, M. Jaskóla, T. Czyzewski, Some aspects of statistical distribution of trace element concentrations in biomedical samples, Nucl Instrum Methods Phys Res b. 150 (1999) 254–259, https://doi.org/10.1016/S0168-583X(98)01058-1.
[26] L. Galluzzi, I. Vitale, S.A. Aaronson, et al, Molecular mechanisms of cell death: recommendations of the Nomenclature Committee on Cell Death 2018, Cell Death & Differentiation 2018 25:3. 25 (2018) 486–541. https://doi.org/10.1038/s41418-017-0012-4.
[27] W. Park, S. Wei, B.S. Kim, B. Kim, S.J. Bae, Y.C. Chae, D. Ryu, K.T. Ha, Diversity and complexity of cell death: a historical review, Experimental & Molecular Medicine 2023 55:8. 55 (2023) 1573–1594. https://doi.org/10.1038/s12276-023-01078-x.